Progress In Electromagnetics Research Letters, Vol. 107, 125–131, 2022

Conjugated Split-Ring Resonators-Based Ultrathin, Polarization- and Angle-Insensitive Metasurface

Evandro César Vilas Boas*, Jorge R. Mejia Salazar, and Felipe A. P. de Figueiredo

Abstract—We show a new polarization- and angle-insensitive ultrathin metasurface design using four conjugated hexagonal split-ring resonators (CHSRRs). The CHSRRs are made of copper and arranged in a $\lambda/4$ cell-size polyimide film substrate with a dielectric constant of 3.5 and thickness of 0.2 mm ($\lambda/400$ at 3.75 GHz). Each CHSRR aperture faces one corner of the square unit cell, thus forming a conjugated loop to achieve TE and TM polarization-insensitive behavior in a wide range of incident angles. Results demonstrated a -10 dB impedance bandwidth of 530 MHz (3.44 to 3.97 GHz) under normal incidence, partially covering the n77 band used for 5G applications.

1. INTRODUCTION

Metasurfaces are two-dimensional metamaterial structures with self-resonant subwavelength elements arranged in one or multiple dielectric layers [1, 2]. This effect comes from coupling individual resonant features of properly placed nearby unit cells (meta-atoms) [2], in analogy to the atoms in a crystalline structure. Indeed, negative permeability, negative permittivity, and non-naturally occurring negative refractive index, i.e., simultaneous negative permeability and permittivity, can be achieved with these artificial materials [3]. Moreover, the meta-atoms can produce abrupt phase changes on the incident electromagnetic wave, allowing for controlling the wave reflection and/or refraction properties [3, 4].

The meta-atoms can be fabricated using all-dielectric, all-metallic, or microstrip line approaches while being periodic or aperiodic arranged according to the desired features/applications [1–3, 5–8]. Regardless of technique, these metasurfaces can consider single-side single-layer, two-side single-layer, or multiple-stacked slab designs. Notably, the latter approach provides more freedom to tailor and tune the electromagnetic properties using robust structures [1, 2]. Furthermore, the unique metasurfaces' electromagnetic characteristics allow for anomalous reflection or refraction through a generalized Snell's law [1]. The physics behind these striking phenomena stems from electric currents induced by the incident electromagnetic waves on the meta-atoms, which strongly depend on the structure geometry and material composition. In addition, reconfigurable techniques provide means to control the induced currents, tailoring the metasurface electromagnetic response [9]. Some recent achievements include lenses, antennas, reconfigurable intelligent surfaces (RIS), absorbers, transmit/reflectarray, RF harvesting devices, and frequency selective surfaces (FSS) designs [1, 2, 7, 8, 10–13].

Specific performance metrics guide the design of metasurface elements, with the frequency response sensitivity to impinging electromagnetic wave polarization and incident angles as recurrent parameters. The metasurface interaction with distinct polarized waves is expected to be insensitive or sensitive. For instance, bifocal Fresnel lenses, antennas, and filters usually exploit the polarization-sensitive frequency or phase response to accomplish the desired device performance [14–16]. On the other hand, several concepts for polarization-insensitive energy harvesting devices, electromagnetic absorbers,

Received 26 August 2022, Accepted 27 October 2022, Scheduled 11 November 2022

* Corresponding author: Evandro César Vilas Boas (evandro.cesar@inatel.br).

The authors are with the Department of Telecommunications Engineering, National Institute of Telecommunication (Instituto Nacional de Telecomunicações, Inatel), Santa Rita do Sapucaí 37540-000, Brazil.

frequency selective surfaces (FSSs), and lenses have been demonstrated [17–20]. Despite all these advances, most polarization-sensitive or -insensitive devices are limited to working under normal incident electromagnetic waves.

Here, we demonstrate a new concept for a nearly omnidirectional metasurface, i.e., our design will reflect the desired wavelength regardless of the incident angle. Our idea is based on conjugated hexagonal split-ring resonators (CHSRRs) comprising four identical hexagonal split-ring resonators placed on a square unit cell. Each CHSRR aperture is aligned with one corner of the unit cell, as illustrated in Figure 1. Although the basic design achieved good polarization-insensitive behavior at transversal electric mode (TE), further modifications were necessary to perform angular stability for the transversal magnetic (TM) incident waves. Moreover, the evolutionary steps and parametric analysis in design from basic polarization-insensitive to incident angle-insensitive metasurfaces are presented. Therefore, we propose a novel technique that may guide the design of future polarization-insensitive and angularly stable reflecting metasurfaces based on conjugated split-ring resonators (SRRs).

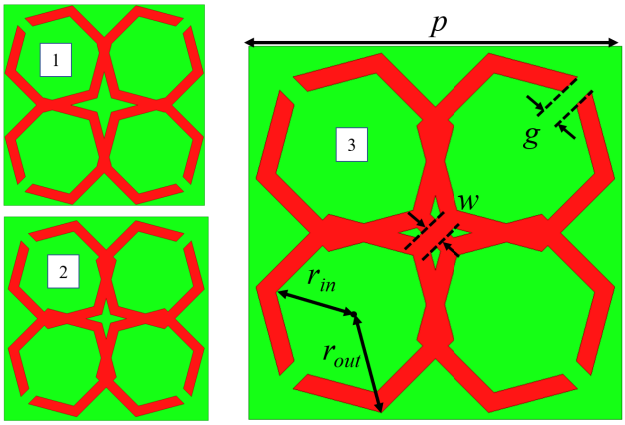

Figure 1. Details of the proposed conjugated hexagonal split-ring resonator structure and cell evolution. Final structure dimensions: $p = 20\,\text{mm}$, $r_{in} = 4.4\,\text{mm}$, $r_{out} = 5.5\,\text{mm}$, $g = 1\,\text{mm}$, and $w = 1\,\text{mm}$.

2. CONJUGATED SPLIT-RING RESONATORS METASURFACES

Split-ring resonators are metallic loops with gaps well-known to provide negative permeability behavior [21, 22]. The structure exhibits effective resonant permeability when an alternating magnetic field is excited, resulting in zero transmission at the desired frequency. The resonant circular currents induce dipole moments, leading to an effective medium with a resonant frequency related to an inductor-capacitor circuit ($\omega_m = 1/\sqrt{LC}$). The SRR-based metasurfaces comprise different arrangements, such as single SRR, complementary SRR, or nested SRR unit cells [23–29].

Single SRRs were used to design a multifunctional metasurface based on a hexagonal shape capable of performing cross and circular polarization conversion at three distinct bands [24]. Double- and multi-gap square SRR (SSRR) structures have been studied regarding magnetic resonance frequency, field, and currents' distributions' behaviors [23, 26]. Meanwhile, nested SRR meta-atoms have been proposed to meet some applications with polarization-insensitive and angular stability requirements. These meta-atoms comprise four SSRRs with a rotational symmetry to achieve TE and TM mode performance metrics [25, 27, 28]. In addition, outer arm connections were introduced to reduce oblique incidence dependence [27, 28]. A nested square SRR has also been exploited by positioning the ring split at the outer cell with a center gap to design absorbers [29].

Regarding the nested SRR, this work exploits this structure in the manner of nested CHSRR to achieve polarization-insensitive and angularly stable performance. The design considered positioning four identical HSRRs made of copper with their aperture facing one corner of the square unit cell while its loops were connected, as seen in Figure 1. The CHSRR structures were arranged in a polyimide film cell of size $\lambda/4$ with a dielectric constant of 3.5 and thickness equal to 0.2 mm ($\lambda/400$ at 3.75 GHz).

3. CONJUGATED HEXAGONAL SRR CELL EVOLUTIONARY STEPS

This section carries out the numerical analysis of the proposed CHSRR cell. Indeed, we chose the ANSYS HFSS simulator tool to design the CHSRR meta-atom and numerically analyze its performance using the Finite Element Method (FEM). The simulator allows for electromagnetic assessing the unit meta-atom structure by applying the Floquet ports and boundaries, which are devoted to planar-periodic structures design. The structure in Figure 1 evolved to present polarization-insensitive and angular stability with the labels identifying the step process. In addition, the meta-atoms performance metrics have been analyzed for the TE and TM modes, as seen in Figure 2 (label 01). The metasurface presented good angular stability ranging from 0 to 60° with polarization-insensitive behavior. However, the structure is susceptible to TM mode polarization with a wide-angle dependence response under oblique incidence. Furthermore, we have modified the cell center to improve these performance metrics for TM mode. First, we cared about improving polarization-insensitive characteristics, which strongly depend on the conjugated-geometry region.

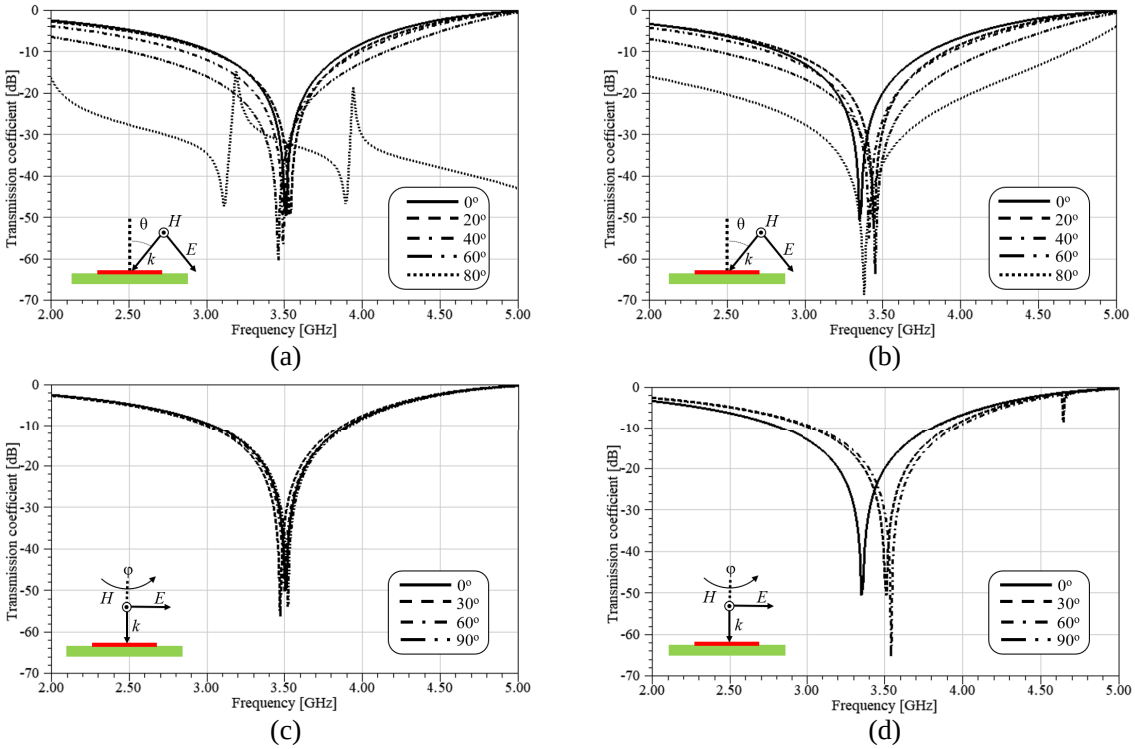

Figure 2. CHSRR initial transmission frequency response: (a) oblique incidence at TE mode, (b) oblique incidence at TM mode, (c) polarization sensitivity at TE mode, (d) polarization sensitivity at TM mode.

The metasurface has demonstrated TM polarization-insensitive by increasing the intersection region of the loop (label 02). This strategy reduced the cell-electrical length and incremented the resonance frequency while the metasurface remained dependent on the oblique incident angles. The design changes introduced a slight shift to the TE mode resonant frequency (less than 1.5%) for different oblique incidence and polarization angles without compromising the performance metrics. Likewise, we inserted diagonal connections at the cell center gap, naturally formed by the conjugated structure. Figure 3 depicts the third CHSRR cell assessment for oblique incident angle and polarization sensitivity, whereas the gap connections accomplished polarization insensitivity and angular stability for TE and TM waves. The TE oblique incidence analysis has presented a 1.3% resonant frequency deviation at 60° compared to the normal incident angle. Similar behavior occurs at an oblique incidence of 80° for the TM mode, with a 2.46% shift in the resonance frequency. However, these results do not compromise the CHSRR

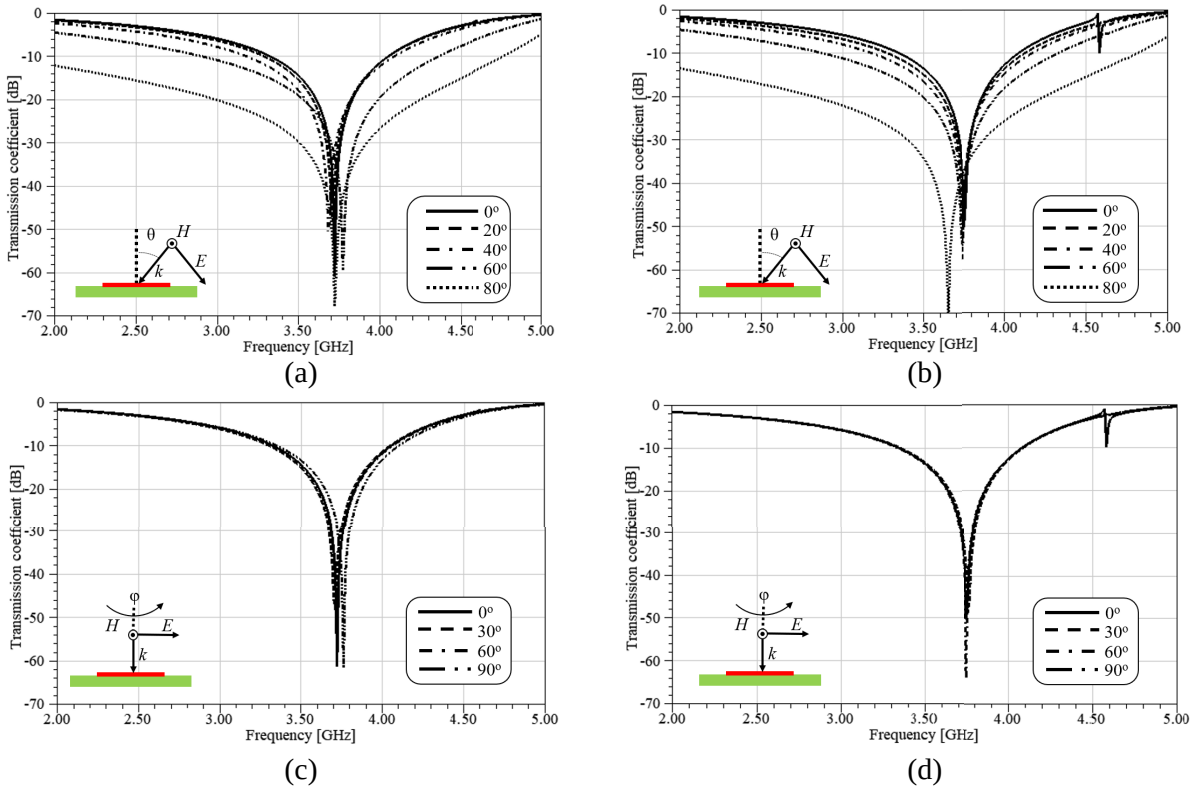

Figure 3. CHSRR final transmission frequency response: (a) oblique incidence at TE mode, (b) oblique incidence at TM mode, (c) polarization sensitivity at TE mode, (d) polarization sensitivity at TM mode.

bandstop transmission bandwidth. On the other hand, a 1.07% shifting in the 60° resonant frequency for the TE polarization sensitivity analysis has been observed, once again, without disturbing the bandstop transmission bandwidth.

Figure 4 shows the diagonal connection effect in the current surface at 3.75 GHz for the three structures excited by the TE and TM modes. The CHSRR has shown an agreement with the expected surface current behavior, which is intense at the opposite part of the split ring [21–23]. Furthermore, the current surface distribution at TE mode is stable for the three structures, which confers a polarization-insensitive characteristic. On the other hand, the TM mode has shown an asymmetric current surface distribution at the first structure center, further corrected by work on modifications in this region. Accordingly, the diagonal connection provided a similar current surface distribution for the TE and TM modes, resulting in a polarization-insensitive and angularly stable CHSRR cell.

4. PERFORMANCE DISCUSSION

Nested SRR structures in Section 2 are claimed as ultrathin metasurfaces. However, the thickness of the slabs is equal to or greater than 0.8 mm, which improves the angular stability and polarization-insensitive metrics for a given cell [25, 27, 29]. Our proposed meta-atom relies on a slab with a thickness equal to 0.2 mm and corresponds to $\lambda/400$ at 3.75 GHz. In addition, an ultrathin nested SRR-based meta-atom using a 0.3 mm thick substrate was proposed in [28]. However, the TM mode bandstop transmission bandwidth strongly depends on the oblique incident angle, with a considerable reduction related to the normal incidence. Regardless of the meta-atom design technique, other works also exploited dielectric slabs with thicknesses equal to or less than 0.3 mm. Furthermore, different substrates have been used to design the metasurface cell in microwave and millimeter-wave bands, aiming at flexible devices for wireless applications. Table 1 compares our meta-atom performance with these metasurface cells.

Table 1. Performance comparison among the proposed CHSRR and other ultrathin meta-atoms.

Ref.	p/λ	t	Pol.-insen.		Ang. stab.		Ref.	p/λ	t	Pol.-insen.		Ang. stab.	
			TE	TM	TE	TM				TE	TM	TE	TM
[28]	0.146	0.300	Yes	Yes	75	75	[32]	0.250	0.125	Yes	Yes	45	45
[30]	0.148	0.254	Yes	Yes	50	75	This work	0.250	0.200	Yes	Yes	**80**	**80**
[31]	0.560	0.125	Yes	Yes	50	75	-						

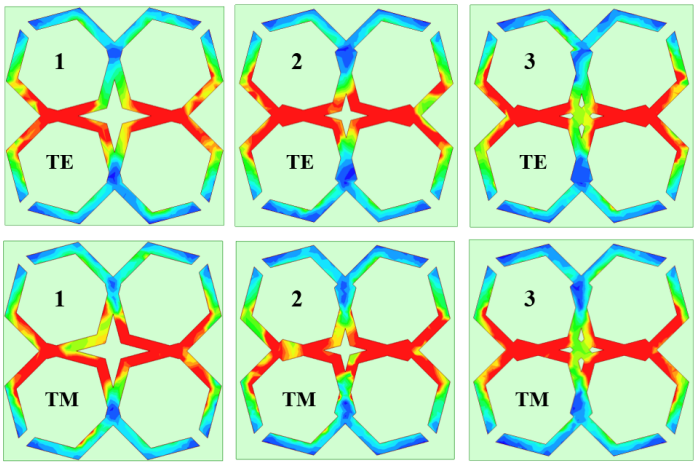

Figure 4. Current distribution for the three cells in Figure 1 at 3.75 GHz.

5. CONCLUSION

We proposed a new technique to accomplish good polarization-insensitive and angularly stable ultrathin metasurface cells for flexible and conformal applications by conjugating a split-ring structure. The copper-based CHSRR structures were arranged in a $\lambda/4$ cell-size polyimide film with a dielectric constant of 3.5 and thickness equal to 0.2 mm ($\lambda/400$ at 3.75 GHz). The -10 dB impedance bandwidth is equal to 530 MHz (3.44 to 3.97 GHz) for a normal incident angle, partially covering the n77 band dedicated to 5G applications. Furthermore, the meta-atoms have shown similar results to other works based on ultrathin-slab design.

ACKNOWLEDGMENT

This work was supported by the National Council for Scientific and Technological Development (CNPq) (403827/2021-3), Fundação de Amparo à Pesquisa do Estado de São Paulo (FAPESP) (2021/06946-0), and partially financed by RNP with resources from MCTIC, grants No. 01245.010604/2020-14, under the Brazil 6G project of the Radiocommunication Reference Center (CRR-Inatel), Brazil.

REFERENCES

1. Bukhari, S. S., J. Y. Vardaxoglou, and W. Whittow, "A metasurfaces review: Definitions and applications," *Appl. Sci.*, Vol. 9, No. 13, 2727, 2019.
2. Glybovski, S. B., S. A. Tretyako, P. A. Belov, Y. S. Kivshar, and C. R. Simovski, "Metasurfaces: From microwaves to visible," *Phy. Rep.*, No. 634, 1–72, 2016.

3. Felbacq, D. and G. Boucitté, *Metamaterials Modelling and Design*, Pan Standford, 2017.
4. Caloz, C. and T. Itoh, *Electromagnetic Metamaterials: Transmission Line Theory and Microwave Applications*, John Wiley & Sons, 2005.
5. Lalbakhsh, A., M. U. Afzal, K. P. Esselle, and S. L. Smith, "Low-cost nonuniform metallic lattice for rectifying aperture near-field of electromagnetic bandgap resonator antennas," *IEEE Trans. Antennas Propag.*, Vol. 68, No. 5, 3328–3335, 2020.
6. Lalbakhsh, A., M. U. Afzal, K. P. Esselle, and S. L. Smith, "A high-gain wideband EBG resonator antenna for 60 GHz unlicenced frequency band," *12th European Conference on Antennas and Propagation (EuCAP 2018)*, 1–3, 2018.
7. Lalbakhsh, A., M. U. Afzal, K. P. Esselle, and S. L. Smith, "All-metal wideband frequency-selective surface bandpass filter for TE and TM polarizations," *IEEE Trans. Antennas Propag.*, Vol. 70, No. 4, 2790–2800, April 2022.
8. Lalbakhsh, A., M. U. Afzal, T. Hayat, K. P. Esselle, and K. Mandal, "All-metal wideband metasurface for near-field transformation of medium-to-high gain electromagnetic sources," *Sci. Rep.*, Vol. 11, Article number: 9421, 2021.
9. He, Q., S. Sun, and L. Zhou, "Tunable/reconfigurable metasurfaces: Physics and applications," *Research*, Vol. 2019, Article ID 1849272, 2019.
10. Esfandiyari, M., A. Lalbakhsh, S. Jarchi, M. G. Miab, H. N. Mahtaj, and R. B. V. B. Simorangkir, "Tunable terahertz filter/antenna-sensor using graphene-based metamaterials," *Materials & Design*, Vol. 220, 110855, 2022.
11. Das, P., K. Mandal, and A. Lalbakhsh, "Beam-steering of microstrip antenna using single-layer FSS based phase-shifting surface," *Int. J. RF. Microw. C. E.*, Vol. 32, No. 3, 23033, 2022.
12. Das, P., K. Mandal, and A. Lalbakhsh, "Single-layer polarization-insensitive frequency selective surface for beam reconfigurability of monopole antennas," *Journal of Electromagnetic Waves and Applications*, Vol. 34, No. 1, 86–102, 2020.
13. Paul, G. S., K. Mandal, and A. Lalbakhsh, "Single-layer ultra-wide stop-band frequency selective surface using interconnected square rings," *AEU — Int. J. Electron. Commun*, Vol. 132, 153630, 2020.
14. Markovich, H., D. Filonov, I. Shishkin, and P. Ginzburg, "Bifocal fresnel lens based on the polarization-sensitive metasurface," *IEEE Trans. Antennas Propag.*, Vol. 66, No. 5, 2650–2654, 2018.
15. Zhao, M., S. Zhu, H. Huang, D. Hu, X. Chen, J. Chen, and A. Zhang, "Frequency-polarization sensitive metasurface antenna for coincidence imaging," *IEEE Antennas Wirel. Propag. Lett.*, Vol. 20, No. 7, 1274–1278, 2021.
16. Peng, C., K. Ou, G. Li, Z. Zhao, X. Li, C. Liu, X. Li, X. Chen, and W. Lu, "Tunable and polarization-sensitive perfect absorber with a phase-gradient heterojunction metasurface in the mid-infrared," *Opt. Express*, Vol. 29, No. 9, 12893–12902, 2021.
17. Yu, F., G. Q. He, X. X. Yang, J. Du, and S. Gao, "Polarization-insensitive metasurface for harvesting electromagnetic energy with high efficiency and frequency stability over wide range of incidence angles," *App. Sci.*, Vol. 10, No. 22, 8047, 2020.
18. Tirkey, M. M. and N. Gupta, "A novel ultrathin checkerboard inspired ultrawideband metasurface absorber," *IEEE Trans. Electromagn. Compat.*, Vol. 64, No. 1, 66–74, 2021.
19. Shukoor, M. A., S. Dey, and S. K. Koul, "A simple polarization-insensitive and wide angular stable circular ring based undeca-band absorber for EMI/EMC applications," *IEEE Trans. Electromagn. Compat.*, Vol. 63, No. 4, 1025–1034, 2021.
20. Xu, H. X., S. Wang, C. Wang, M. Wang, Y. Wang, and Q. Peng, "Polarization-insensitive metalens and its applications to reflectarrays with polarization diversity," *IEEE Trans. Antennas Propag.*, Vol. 70, No. 3, 1895–1905, 2021.
21. Hesmer, F., E. Tatartschuk, O. Zhuromskyy, A. A. Radkovskaya, M. Shamonin, T. Hao, C. J. Stevens, G. Faulkner, D. J. Edwards, and E. Shamonina, "Coupling mechanisms for split ring resonators: Theory and experiment," *Phys. Status Solidi B*, Vol. 244, No. 4, 1170–1175, 2007.

22. Jakšić, Z., S. Vuković, J. Matovic, and D.Tanaslović, "Negative refractive index metasurfaces for enhanced biosensing," *Materials*, Vol. 4, No. 1, 1–36, 2010.
23. Penciu, R. S., K. Aydin, M. Kafesaki, Th. Koschny, E. Ozbay, E. N. Economou, and C. M. Soukoulis, "Multi-gap individual and coupled split-ring resonator structures," *Opt. Express*, Vol. 16, No. 22, 18131–18144, 2018.
24. Wahidi, M. S., M. I. Khan, F. A. Tahir, and H. Rmili, "Multifunctional single layer metasurface based on hexagonal split ring resonator," *IEEE Access*, Vol. 8, 28054–28063, 2020.
25. Zhong, H. T., X. X. Yang, C. Tan, and K. Yu, "Triple-band polarization-insensitive and wide-angle metamaterial array for electromagnetic energy harvesting," *Appl. Phys. Lett.*, Vol. 109, No. 25, 253904, 2016.
26. Miyamaru, F., S. Kubota, T. Nakanishi, S. Kawashima, N. Sato, M. Kitano, and M. W. Takeda, "Transmission properties of double-gap asymmetric split ring resonators in terahertz region," *Appl. Phys. Lett.*, Vol. 101, No. 5, 051112, 2012.
27. Assimonis, S. D. and V. Fusco, "Polarization insensitive, wide-angle, ultra-wideband, flexible, resistively loaded, electromagnetic metamaterial absorber using conventional iinkjet-printing technology," *Sci. Rep.*, Vol. 9, No. 1, 1–15, 2019.
28. Bhope, V. and A. Harish, "A novel bandstop frequency selective surface using coupled split ring resonators," *2019 IEEE Asia-Pacific Microwave Conference (APMC)*, 1745–1747, IEEE, 2019.
29. Mol, V. L. and C. Aanandan, "An ultrathin microwave metamaterial absorber with enhanced bandwidth and angular stability," *J. Phys. Commun.*, Vol. 1, No. 1, 015003, 2017.
30. Ghaneizadeh, A., M. Joodaki, J. Börcsök, A. Golmakani, and K. Mafinezhad, "Analysis, design, and implementation of a new extremely ultrathin 2-D-isotropic flexible energy harvester using symmetric patch FSS," *IEEE Trans. Microw. Theory Techn.*, Vol. 68, No. 6, 2108–2115, 2020.
31. Jilani, S. F., O. P. Falade, T. Wildsmith, P. Reip, and A. Alomainy, "A 60-GHz ultra-thin and flexible metasurface for frequency-selective wireless applications," *App. Sci.*, Vol. 9, No. 5, 945, 2019.
32. Yong, W. Y., S. K. A. Rahim, M. Himdi, F. C. Seman, D. L. Suong, M. R. Ramli, and H. A. Elmobarak, "Flexible convoluted ring shaped FSS for X-band screening application," *IEEE Access*, Vol. 6, 11657–11665, 2018.